The structures of marialite (Me_6) and meionite (Me_{93}) in space groups $P4_2/n$ and $I4/m$, and the absence of phase transitions in the scapolite series

Sytle M. Antao[a]
Department of Geoscience, University of Calgary, Calgary, Alberta T2N 1N4, Canada
Ishmael Hassan
Department of Chemistry, University of the West Indies, Mona, Kingston 7, Jamaica

(Received 26 January 2011; accepted 2 February 2011)

The crystal structures of marialite (Me_6) from Badakhshan, Afghanistan and meionite (Me_{93}) from Mt. Vesuvius, Italy were obtained using synchrotron high-resolution powder X-ray diffraction (HRPXRD) data and Rietveld structure refinements. Their structures were refined in space groups $I4/m$ and $P4_2/n$, and similar results were obtained. The Me_6 sample has a formula $Ca_{0.24}Na_{3.37}K_{0.24}[Al_{3.16}Si_{8.84}O_{24}]Cl_{0.84}(CO_3)_{0.15}$, and its unit-cell parameters are $a=12.047555(7)$, $c=7.563210(6)$ Å, and $V=1097.751(1)$ Å^3. The average ⟨T1-O⟩ distances are 1.599(1) Å in $I4/m$ and 1.600(2) Å in $P4_2/n$, indicating that the T1 site contains only Si atoms. In $P4_2/n$, the average distances of ⟨T2-O⟩=1.655(2) and ⟨T3-O⟩=1.664(2) Å are distinct and are not equal to each other. However, the mean ⟨T2,3-O⟩=1.659(2) Å in $P4_2/n$ and is identical to the ⟨T2′-O⟩=1.659(1) Å in $I4/m$. The ⟨M-O⟩ [7]=2.754(1) Å (M site is coordinated to seven framework O atoms) and M-A=2.914(1) Å; these distances are identical in both space groups. The Me_{93} sample has a formula of $Na_{0.29}Ca_{3.76}[Al_{5.54}Si_{6.46}O_{24}]Cl_{0.05}(SO_4)_{0.02}(CO_3)_{0.93}$, and its unit-cell parameters are $a=12.19882(1)$, $c=7.576954(8)$ Å, and $V=1127.535(2)$ Å^3. A similar examination of the Me_{93} sample also shows that both space groups give similar results; however, the C–O distance is more reasonable in $P4_2/n$ than in $I4/m$. Refining the scapolite structure near Me_0 or Me_{100} in $I4/m$ forces the T2 and T3 sites (both with multiplicity 8 in $P4_2/n$) to be equivalent and form the T2′ site (with multiplicity 16 in $I4/m$), but ⟨T2-O⟩ is not equal to ⟨T3-O⟩ in $P4_2/n$. Using different space groups for different regions across the series implies phase transitions, which do not occur in the scapolite series. © *2011 International Centre for Diffraction Data.* [DOI: 10.1154/1.3582802]

Key words: marialite, meionite, crystal structure, HRPXRD, phase transition

I. INTRODUCTION

Scapolite forms solid solutions between the end members marialite, $Na_4[Al_3Si_9O_{24}]Cl=Me_0$ and meionite, $Ca_4[Al_6Si_6O_{24}]CO_3=Me_{100}$. Scapolite forms two series that meet at Me_{75}, $Na_2Ca_6[Al_{10}Si_{14}O_{48}](CO_3)_2$, and the composition varies by replacement of $[Na_4\cdot Cl]Si_2$ for $[NaCa_3\cdot CO_3]Al_2$ between Me_{0-75}, and by the replacement of $[NaCa_3\cdot CO_3]Si$ for $[Ca_4\cdot CO_3]Al$ between Me_{75-100} (Evans *et al.*, 1969; Hassan and Buseck, 1988; Deer *et al.*, 1992). In addition, chemical analyses of scapolite are represented by two straight lines that meet at Me_{75}, again indicating two series (see Figure 12 in Hassan and Buseck, 1988 or Figure 188 in Deer *et al.*, 1992). The Ca–Na cations disordered on heating, but the $Cl-CO_3$ order remains to 900 °C (Antao and Hassan, 2002, 2008a, 2008b).

A number of studies on scapolite divided the series into three subseries that meet at Me_{20-25} and Me_{60-67} (e.g., Sokolova *et al.*, 1996, 2000; Teertstra and Sherriff, 1996; Zolotarev 1996; Zolotarev *et al.*, 2003; Sherriff *et al.*, 1998, 2000; Teertstra *et al.*, 1999; Hawthorne and Sokolova, 2008; Sokolova and Hawthorne, 2008). Ulbrich (1973a) suggested a break in cell parameters at Me_{65-66} (his Figure 1).

Using transmission electron microscopy (TEM), and the type-b reflections ($h+k+l=$odd), three subseries were identified: series Me_{0-18} and Me_{90-100} have space group $I4/m$, whereas series Me_{18-90} has space group $P4_2/n$ (Seto *et al.*, 2004). Some scapolite samples were refined in both space groups $I4/m$ and $P4_2/n$, for example, ON8 (Me_{21}) and ON45 (Me_{93}) samples do not show type-b reflections, but that does not mean that they are body centered (Lin and Burley, 1973c). These authors indicated that the type-b reflections are less intense than the detection limit of the X-ray experiments and suggested that all scapolite structures belong to space group $P4_2/n$, except the end members, Me_0 and Me_{100}, which do not occur naturally.

In space group $P4_2/n$, the T2 and T3 tetrahedra are symmetrically distinct and are not required to have equal ⟨T2-O⟩ and ⟨T3-O⟩ distances (Figure 1). Each of the T2 and T3 sites with a multiplicity of 8 in the $P4_2/n$ structure is symmetrically distinct, and together they form the T2′ site with a multiplicity of 16 in space group $I4/m$. Sokolova and Hawthorne (2008) refined the structures of their S15 sample ($Me_{76.9}$) in both space groups, $I4/m$ and $P4_2/n$. They test for the best space group for S15 by comparing the ⟨T2-O⟩ and ⟨T3-O⟩ distances in the $P4_2/n$ refinement. If these distances are equal, the space group is $I4/m$; if these distances are not equal, the space group is $P4_2/n$. Their relevant distances are 1.691(2) and 1.666(2) Å, so they assign the space group

---

[a] Author to whom correspondence should be addressed. Electronic mail: antao@ucalgary.ca

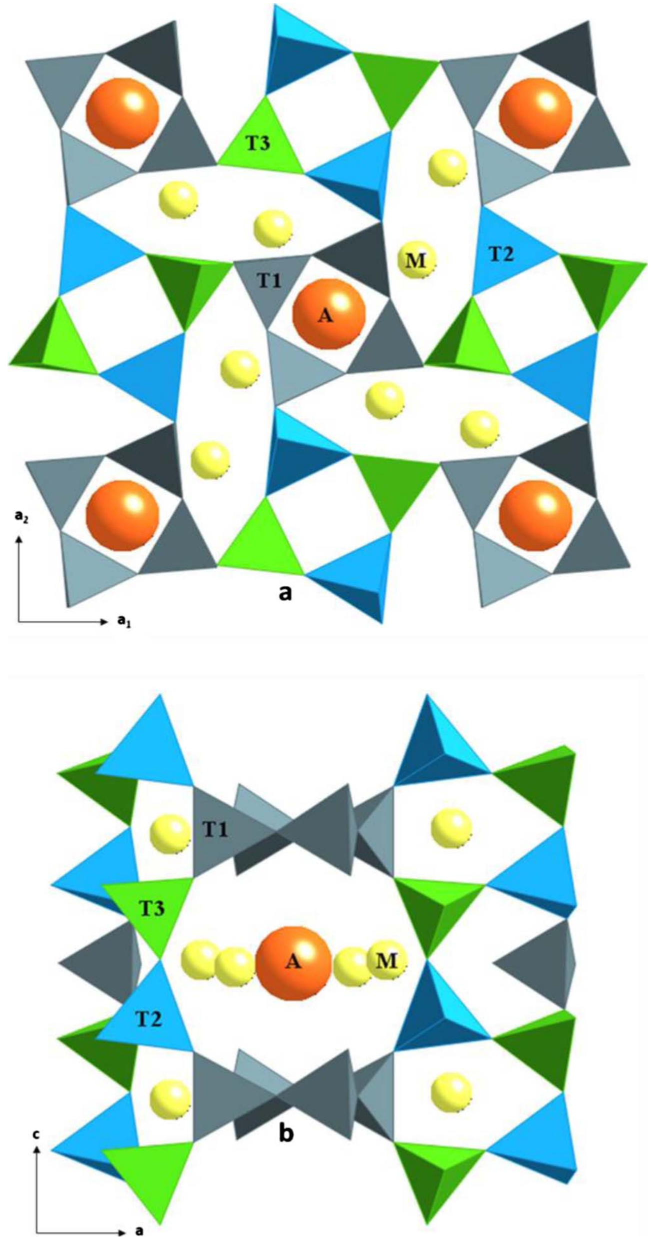

Figure 1. (Color online) (a) Scapolite structure showing framework T and interstitial M and A sites, four-membered rings, and oval shaped channels. (b) A cage containing A and M ions and uncommon five-membered rings; A is coordinated by four M in a square-planar configuration. Space group $P4_2/n$.

$P4_2/n$ to sample S15. In spite of refining their S15 sample ($Me_{76.9}$) in space group $P4_2/n$, Sokolova and Hawthorne (2008) claimed a phase transition at $Me_{60\text{–}67}$ based on a break in the c-cell parameters. Furthermore, they refined other samples close to Me_0 and Me_{100} in space group $I4/m$, thereby implying two phase transitions with an intermediate series that is refined in space group $P4_2/n$.

Hassan and Antao (2010) observed a discontinuity in unit-cell parameters at Me_{75} and the absence of any phase transition across the scapolite series; a maximum in the c parameter occurs at $Me_{37.5}$. In this study, the structures of a marialite (Me_6) and a meionite (Me_{93}) sample were refined in both space groups $I4/m$ and $P4_2/n$, and similar results were obtained. There is no reason for phase transitions at $Me_{20\text{–}25}$, $Me_{60\text{–}67}$, or Me_{75} and no reason to refine the structure near Me_0 and Me_{100} in the higher symmetry space group $I4/m$, thereby forcing the T2 and T3 sites in $P4_2/n$ to be the same and constitute the T2′ site in $I4/m$.

The structure of scapolite was determined by Pauling (1930) and Schiebold and Seumel (1932) and refined by several researchers in either space group $I4/m$ or $P4_2/n$ (Papike and Zoltai, 1965; Papike and Stephenson, 1966; Lin and Burley, 1973a, 1973b, 1973c, 1974; Ulbrich, 1973b; Levien and Papike, 1976; Peterson *et al.*, 1979; Aitken *et al.*, 1984; Comodi *et al.*, 1990; Belokoneva *et al.*, 1991, 1993; Teertstra *et al.*, 1999; Sokolova and Hawthorne, 2008). More data were obtained using Rietveld refinement and MAS NMR spectroscopy (Sokolova *et al.*, 1996, 2000; Sherriff *et al.*, 1998, 2000), valence-matching principle (Hawthorne and Sokolova 2008), and electrostatic energy calculations (Chamberlain *et al.*, 1985). A review of scapolite crystal chemistry was given by Lin (1975).

II. EXPERIMENTAL

A marialite sample from Badakhshan, Afghanistan and a meionite sample from Mt. Vesuvius, Italy were used in this study. The marialite crystals are large ($0.5 \times 0.5 \times 0.5$ cm^3), purple in color, and are of gem quality. The meionite crystal is colorless and was obtained from the Smithsonian National Museum of Natural History (B20018-1). Their chemical analyses were obtained by electron microprobe. The crystals are homogeneous based on optical observation and microprobe data. The chemical composition for the marialite sample is $K_{0.24}Na_{3.37}Ca_{0.24}[Al_{3.16}Si_{8.84}O_{24}]Cl_{0.84}(SO_4)_{0.02}(CO_3)_{0.15}$ and corresponds to $Me_{6.2}$; the meionite sample is $Na_{0.29}Ca_{3.76}[Al_{5.54}Si_{6.46}O_{24}]Cl_{0.05}(SO_4)_{0.02}(CO_3)_{0.93}$ and corresponds to $Me_{92.9}$.

A small (about $0.2 \times 0.2 \times 0.2$ mm^3) crystal was hand-picked under a binocular microscope and finely crushed in an agate mortar and pestle for synchrotron high-resolution powder X-ray diffraction (HRPXRD) experiments that were performed at beamline 11-BM, Advanced Photon Source, Argonne National Laboratory. The sample was loaded into a Kapton capillary and rotated during the experiment at a rate of 90 rotations/s. The data were collected to a maximum 2θ of about 40° with a step time of 0.1 s per step. The step size was 0.001° and 0.0005° for Me_6 and Me_{93}, respectively. Additional details of the experimental set-up are given elsewhere (Antao *et al.*, 2008; Lee *et al.*, 2008; Wang *et al.*, 2008).

The HRPXRD method, instead of the single-crystal method, was chosen because it is rapid (about 1 h for a data set), it provides superior cell parameters, and bond-distances and angles that are comparable to those obtained by the single-crystal method. Weak reflections, including satellite reflections, are easily observed because of the high beam intensity of synchrotron X-rays. In addition, single-crystal data are available to compare with our present HRPXRD data. Moreover, Antao *et al.* (2008) compared data from HRPXRD and single-crystal methods for several minerals and showed that the results are comparable.

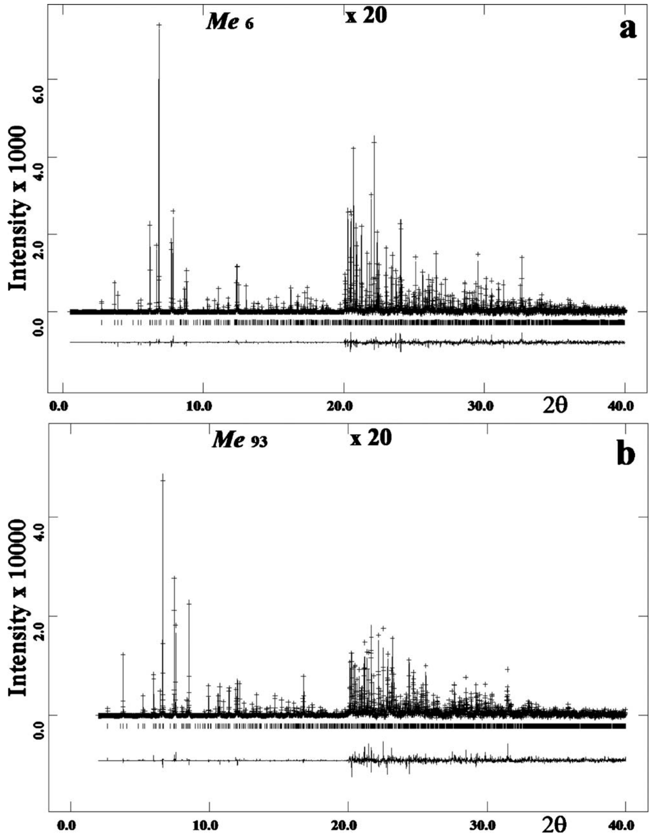

Figure 2. HRPXRD traces for (a) marialite, Me_6, and (b) meionite, Me_{93}, in space group $P4_2/n$ together with the calculated (continuous line) and observed (crosses) profiles. The difference curves (*Iobs–Icalc*) are shown at the bottom. The short vertical lines indicate allowed reflection positions. The traces beyond 20° 2θ are scaled by 20x.

TABLE I. Refinement data for marialite (Me_6) and meionite (Me_{93}).

	Me_6		Me_{93}	
	$I4/m$	$P4_2/n$	$I4/m$	$P4_2/n$
χ^2	2.100	2.071	2.679	2.684
$R_F{}^2$	0.0752	0.0724	0.0713	0.0674
N_{obs}	1429	2680	1594	3006
2θ range (deg)	2.5–40	2.5–40	2.5–40	2.5–40
λ (Å)	0.41226(2)	0.41226(2)	0.40243(2)	0.40243(2)
Step size (°2θ)	0.001	0.001	0.0005	0.0005
No. of data pts.	37499	37499	73227	73227
a (Å)	12.047554(7)	12.047555(7)	12.19882(1)	12.19882(1)
c (Å)	7.563210(6)	7.563210(6)	7.576955(8)	7.576954(8)
V (Å^3)	1097.751(1)	1097.751(1)	1127.537(2)	1127.535(2)
Me ^{a} (%)	6.2	6.2	92.9	92.9

[a] From electron microprobe chemical analyses; $Me(\%)=[\mathrm{Ca}/(\mathrm{Ca}+\mathrm{Na}+\mathrm{K})]\times 100$.

III. RIETVELD STRUCTURE REFINEMENT

The crystal structure of marialite was modeled using the Rietveld method (Rietveld, 1969) that is incorporated in the GSAS program (Larson and Von Dreele, 2000) and using the EXPGUI interface (Toby, 2001). Initial structural parameters were taken from Teertstra *et al.* (1999). The structure refinement was carried out by varying parameters in the following sequence: scale factor, background, cell, zero shift, profile, atom positions, and isotropic displacement parameters. Finally, all variables were refined simultaneously until convergence was achieved. Site occupancy factors for the *M* cations and *A* anions were fixed to that obtained by chemical analyses. We assumed that the *A* anions completely occupy the $4/m$ site, the disordered trigonal CO_3 group occurs in a small quantity, so its O atoms were not modeled in the refinement for marialite, but they occur in significant quantity in meionite, where they are modeled quite well. Figures 2(a) and 2(b) display the HRPXRD trace for marialite, Me_6 and meionite, Me_{93}, respectively. Table I contains the refinement statistics and unit-cell parameters. Table II contains the atom positions and isotropic displacement parameters, *U*. Table III contains selected bond-distances and angles.

IV. RESULTS AND DISCUSSION

A. Marialite (Me_6)

The unit-cell parameters for marialite are $a=12.047555(7)$ Å, $c=7.563210(6)$ Å, and $V=1097.751(1)$ Å^3. Sample S2 (Me_7) from Sokolova and Hawthorne (2008) has $a=12.0541(5)$ Å, $c=7.5682(3)$ Å, and $V=1099.7(1)$ Å^3. The differences between S2 and our sample are 0.007 Å for *a*, 0.005 Å for *c*, and 1.95 Å^3 for *V*.

The refined marialite structures in both space groups $I4/m$ and $P4_2/n$ gave identical results (Table III). The average ⟨T1-O⟩ distances are 1.599(1) and 1.600(2) Å for space groups $I4/m$ and $P4_2/n$, respectively. Therefore, the T1 site contains only Si atoms. The average ⟨T2′-O⟩=1.659(1) Å in space group $I4/m$ and is identical to the mean of ⟨T2-O⟩ =1.655(2) and ⟨T3-O⟩=1.664(2) Å, which is 1.659(2) Å (=⟨T2,3-O⟩) for the lower symmetry space group $P4_2/n$. The distinct T2 and T3 sites are not identical in space group $P4_2/n$; they do not have identical ⟨T-O⟩ distances. The T2 and T3 sites are forced to be a T2′ site in space group $I4/m$. The Al–Si atoms are disordered in the T2 and T3 sites in space group $P4_2/n$, and the T2′ site in space group $I4/m$. The ⟨M-O⟩[7] (M site is coordinated to seven framework O atoms) and M-A distances are identical in both space groups (Table III). The structure in space group $I4/m$ has a smaller number of observed reflections, $N_{obs}=1429$, whereas in space group $P4_2/n$, $N_{obs}=2680$; nearly twice as many reflections (the type-b reflections are very weak towards Me_0 and Me_{100}). The structural results for marialite in space groups $I4/m$ and $P4_2/n$ are identical, but the ⟨T2-O⟩ and ⟨T3-O⟩ distances are not equal. Therefore, the $P4_2/n$ space group is preferred and there is no reason for a phase transition at Me_{20-25}.

The S2 sample (Me_7) from Sokolova and Hawthorne (2008) in space group $I4/m$ has ⟨T1-O⟩=1.607 Å and ⟨T2′-O⟩=1.662 Å, which are similar to our values given above for the same space group $I4/m$. Their ⟨M-O⟩[7] =2.736 Å and M-A=2.945(1) Å, whereas we obtained 2.754(2) Å and 2.914(1) Å, respectively, for both space groups (Table III). The difference between these ⟨M-O⟩[7] distances is 0.018 Å and between the M-A distances is 0.031 Å.

In sodalite, $Na_8[Si_6Al_6O_{24}]Cl_2$, each Cl atom is surrounded by four Na atoms in a tetrahedral configuration and Na–Cl=2.7337(4) Å (Hassan and Grundy, 1984; Hassan *et al.*, 2004; Antao *et al.*, 2008). In marialite, each Cl atom is

TABLE II. Atom positions and U (Å^2) for marialite (Me_6) and meionite (Me_{93}).

$I4/m$		Me_6	Me_{93}
T1	x	0.16191(6)	0.16095(5)
	y	0.08945(5)	0.09296(5)
	z	0	0
	U	0.0090(1)	0.0101(1)
T2	x	0.16247(4)	0.15972(4)
	y	0.41535(4)	0.41342(3)
	z	0.20652(5)	0.20701(5)
	U	0.0114(1)	0.0122(1)
O1	X	0.0433(1)	0.0420(1)
	Y	0.1472(1)	0.15166(9)
	z	0	0
	U	0.0181(4)	0.0241(4)
O2	x	0.1943(1)	0.18656(9)
	y	0.3822(1)	0.37567(8)
	z	0	0
	U	0.0139(4)	0.0161(4)
O3	x	0.44825(8)	0.45047(7)
	y	0.15010(8)	0.14988(6)
	z	0.2171(1)	0.2076(1)
	U	0.0217(3)	0.0210(3)
O4	x	0.27037(8)	0.26520(6)
	y	0.37309(7)	0.36603(6)
	z	0.6717(1)	0.6762(1)
	U	0.0196(3)	0.0271(3)
M[a]	X	0.37211(9)	0.35739(4)
	Y	0.29485(9)	0.28175(4)
	z	0	0
	U	0.0402(3)	0.0285(1)
A[b]	x	1/2	1/2
	y	1/2	1/2
	z	0	0
	U	0.0383(5)	0.0887(9)
O5C	x	-	0.6030(1)
	y	-	0.5126(3)
	z	-	0
	U	-	0.0887(9)

$P4_2/n$		Me_6	Me_{93}
T1	x	0.58813(6)	0.58907(5)
	y	0.66053(5)	0.65706(5)
	z	0.2487(3)	0.2478(3)
	U	0.0091(1)	0.0101(1)
T2	x	0.9130(2)	0.9078(1)
	y	0.1640(2)	0.1635(1)
	z	0.0426(3)	0.0424(3)
	U	0.0091(1)	0.0096(1)
T3	x	0.6666(2)	0.6634(1)
	y	0.0880(2)	0.0886(1)
	z	0.9558(3)	0.9565(2)
	U	0.0091(1)	0.0096(1)
O1	x	0.7067(1)	0.7081(1)
	y	0.6027(1)	0.59820(9)
	z	0.2533(6)	0.2535(5)
	U	0.0179(4)	0.0233(4)
O2	x	0.9443(1)	0.93665(9)
	y	0.1321(1)	0.12565(8)
	z	0.2478(6)	0.2454(5)
	U	0.0141(4)	0.0158(4)
O3	x	0.6007(4)	0.6009(2)
	y	0.1988(4)	0.2010(2)
	z	0.0328(4)	0.0423(4)
	U	0.021(1)	0.0241(2)
O4	x	0.8024(4)	0.7997(2)
	y	0.0991(4)	0.0993(2)
	z	0.9666(4)	0.9576(4)
	U	0.022(2)	0.0241(2)
O5	x	0.5231(3)	0.5213(2)
	y	0.6265(4)	0.6155(2)
	z	0.0761(5)	0.0729(3)
	U	0.016(1)	0.0241(2)
O6	x	0.6201(4)	0.6164(2)
	y	0.9825(3)	0.9911(2)
	z	0.0803(4)	0.0748(3)
	U	0.020(1)	0.0241(2)
M	x	0.62206(8)	0.60734(4)
	y	0.54477(9)	0.53171(4)
	z	0.7427(4)	0.7417(1)
	U	0.0390(3)	0.0275(2)
A	x	3/4	3/4
	y	3/4	3/4
	z	3/4	3/4
	U	0.0404(5)	0.092(1)
O7C	x		0.8543(1)
	y		0.7627(3)
	z		0.7627(11)
	U		0.092(1)

[a] M=(Ca,Na,K).

[b] A=(Cl,C,S).

also surrounded by four Na atoms in a square-planar configuration and Na–Cl=2.914(1) Å. Repulsion of the Na atoms in the square-planar configuration causes the Na–Cl distance to be larger in marialite compared to that in sodalite.

B. Meionite (*Me*$_{93}$)

The unit-cell parameters for meionite ($Me_{92.9}$) are a =12.19882(1) Å, c=7.576954(8) Å, and V =1127.535(2) Å^3. Sample S18 ($Me_{92.8}$) from Sokolova and Hawthorne (2008) for a sample from the same locality has a=12.2077(5) Å, c=7.5832(3) Å, and V=1130.1(1) Å^3. The differences between S18 and our sample are 0.0089 Å

TABLE III. Bond distances (Å) and angles (deg) for marialite (Me_6) and meionite (Me_{93}).

$I4/m$	Me_6	Me_{93}
T1-O1	1.590(2)	1.618(1)
T1-O1′	1.609(2)	1.650(1)
T1-O4	1.599(1)	1.6862(8)
T1-O4′	1.599(1)	1.6862(8)
⟨T1-O⟩	**1.599(1)**	**1.660(1)**
T2′-O2	1.6572(6)	1.6672(5)
T2′-O3	1.652(1)	1.6647(8)
T2′-O3′	1.654(1)	1.6798(8)
T2′-O4	1.673(1)	1.6654(8)
⟨T2′-O⟩	**1.659(1)**	**1.669(1)**
Mean T	**1.639(1)**	**1.666(1)**
M-O2	2.387(2)	2.378(1)
M-O3 × 2	2.565(1)	2.5203(8)
M-O4 × 2	2.925(1)	2.8884(9)
M-O4′ × 2	2.954(1)	2.6958(8)
⟨M-O⟩[7]	**2.753(1)**	**2.655(1)**
M-O5C	-	2.555(3)
M-O5C′	-	2.359(3)
⟨M-O⟩[9]	**-**	2.611(2)
M-A	**2.913(1)**	**3.1804(5)**
C–O × 4		1.266(2)
T1-O1-T1	160.3(1)	157.67(9)
T2′-O2-T2′	140.97(8)	140.38(6)
T2′-O3-T2′	149.56(7)	146.35(5)
T1-O4-T2′	139.29(7)	136.93(5)
⟨T-O-T⟩	147.54(3)	145.33(4)

$P4_2/n$	Me_6	Me_{93}
T1-O1	1.589(2)	1.620(1)
T1-O1′	1.610(2)	1.649(1)
T1-O5	1.576(4)	1.642(3)
T1-O6	1.623(4)	1.735(3)
⟨T1-O⟩	**1.600(2)**	**1.661(1)**
T2-O2	1.643(4)	1.644(3)
T2-O3	1.662(5)	1.656(3)
T2-O4	1.649(5)	1.663(3)
T2-O5	1.665(5)	1.739(2)
⟨T2-O⟩	**1.655(2)**	**1.675(1)**
T3-O2	1.673(4)	1.693(3)
T3-O3	1.659(5)	1.698(3)
T3-O4	1.643(5)	1.668(3)
T3-O6	1.679(4)	1.597(2)
⟨T3-O⟩	**1.664(2)**	**1.664(1)**
⟨T2,3-O⟩	**1.659(2)**	**1.670(1)**
Mean T	**1.639(1)**	**1.667(1)**
M-O2	2.388(2)	2.379(1)
M-O3	2.539(5)	2.490(3)
M-O4	2.589(5)	2.553(3)
M-O5	2.958(5)	2.906(3)
M-O5′	3.032(5)	2.768(3)
M-O6	2.878(4)	2.622(3)
M-O6′	2.894(5)	2.874(3)
⟨M-O⟩[7]	**2.754(2)**	**2.656(1)**
M-O7C	-	2.557(3)
M-O7C′	-	2.351(3)
⟨M-O⟩[9]	-	2.611(2)
M-A	**2.914(1)**	**3.1817(5)**
C–O × 4		1.285(2)
T1-O1-T1	160.1(1)	157.47(9)
T2-O2-T3	140.99(8)	140.21(6)
T2-O3-T3	149.7(3)	146.6(2)
T2-O4-T3	149.4(3)	146.1(2)
T1-O5-T2	140.5(3)	134.6(2)
T1-O6-T3	138.1(3)	138.8(2)
⟨T-O-T⟩	146.5(1)	143.95(7)

In space group $P4_2/n$, ⟨T2,3-O⟩=[⟨T2-O⟩+⟨T3-O⟩]/2 and mean T=[⟨T1-O⟩+⟨T2-O⟩+⟨T3-O⟩]/3. In space group $I4/m$, the mean T=[⟨T1-O⟩+(2×⟨T2′-O⟩)]/3.

for a, 0.0062 Å for c, and 2.57 Å^3 for V. Although these samples are from the same locality and have similar composition, our cell parameters are different from those reported by Sokolova and Hawthorne (2008).

The refined meionite structure in both space groups $I4/m$ and $P4_2/n$ gave similar results (Table III). The average ⟨T1-O⟩ distances are 1.660(1) Å and 1.661(1) Å for space groups $I4/m$ and $P4_2/n$, respectively. Therefore, the Al and Si atoms are partially disordered in the T1 site. The average ⟨T2′-O⟩=1.669(1) Å in space group $I4/m$, and is identical to the mean of ⟨T2-O⟩=1.675(1) and ⟨T3-O⟩=1.664(1) Å, which is ⟨T2,3-O⟩=1.670(1) Å for space group $P4_2/n$. Based on ⟨T-O⟩ distances, the Al–Si order in the distinct T2 and T3 sites are not identical in space group $P4_2/n$. The Al–Si atoms are partially disordered in the T2 and T3 sites in space group $P4_2/n$, and the T2′ site in space group $I4/m$. The ⟨M-O⟩[7] and M-A distances are identical in both space groups (Table III). For the disordered CO_3 group, a more reasonable C–O distance is obtained in space group $P4_2/n$ compared to $I4/m$. The structural results for meionite in space groups $I4/m$ and $P4_2/n$ are similar, so there is no reason for a phase transition at Me_{60-67} and have the structure in the higher symmetry space group $I4/m$. The meionite structure in space group $I4/m$ has the number of observed reflections, $N_{obs}=1594$, whereas in space group $P4_2/n$, $N_{obs}=3006$; nearly twice as many reflections (the type-b reflections are very weak toward Me_{93}). Refinement of the structure in the lower symmetry space group $P4_2/n$ shows that the T2 and T3 sites are not equivalent. In Me_6, ⟨T2-O⟩ is slightly lesser than ⟨T3-O⟩, whereas in Me_{93}, ⟨T2-O⟩ is slightly greater than ⟨T3-O⟩ (Table III).

The S18 sample ($Me_{92.8}$) from Sokolova and Hawthorne (2008) has ⟨T1-O⟩=1.658 Å and ⟨T2′-O⟩=1.683 Å, compared to our ⟨T1-O⟩=1.660(1) Å and ⟨T2′-O⟩ =1.669(1) Å in space group $I4/m$. Their ⟨M-O⟩[7] =2.639 Å and M-A=3.196(1) Å, whereas we obtained 2.655(1) Å and 3.1804(5) Å, respectively, for both space groups (Table III). The difference between these respective ⟨M-O⟩[7] and M-A distances is 0.016 Å for both, and probably arise from the different cell parameters used.

Why are the type-b reflections unobserved near Me_0 and Me_{100}? The simple answer is that they are too weak to be observed. Lin and Burley (1973c) did not observe type-b reflections in their ON8 (Me_{21}) and ON45 (Me_{93}) samples, but they refined the structure of these samples in both space groups. With TEM, type-b reflections were observed between Me_{18-90} (Seto *et al.*, 2004). Phakey and Ghose (1972) and Hassan and Buseck (1988) showed that type-b reflections arise from $Cl-CO_3$ order, instead of Al–Si order, and give rise to antiphase domain boundaries (APBs). Complete order of $Cl-CO_3$ is achieved where their ratio is 1:1, which occurs at $Me_{37.5}$, $[Na_5Ca_3[Al_8Si_{16}O_{48}]Cl(CO_3)]$ (Hassan and Buseck, 1988). For the Me_6 sample, the amounts of Cl and CO_3 are 0.84 and 0.15, respectively. This means that 0.15 CO_3 can couple with 0.15 Cl to form an ordered distribution, whereas the remaining 0.69 Cl are distributed randomly throughout the structure. This 0.15 CO_3–0.15 Cl order distribution occurs in small domains (about 15% of the sample). Only if such small domains are observed by TEM, then the type-b reflections may be observed in a high-voltage TEM. The chance of observing such small domains becomes challenging toward Me_0, but they are easily observed at $Me_{37.5}$, where 1:1 $Cl-CO_3$ order occurs throughout the crystal (Hassan and Buseck, 1988). Using high-resolution transmission electron microscopy (HRTEM), domains from series-1 scapolite (Me_{0-75}) were observed as inclusions in series-2 scapolite (Me_{75-100}), so type-b reflections were observed in a $Me_{79.6}$ scapolite sample, but a discontinuity in cell parameters and composition occurs at Me_{75}, $[Na_2Ca_6[Al_{10}Si_{14}O_{48}](CO_3)_2]$, where the A site is completely filled with CO_3 groups from Me_{75-100} (Hassan and Buseck, 1988; Hassan and Antao, 2010). Scapolite analyses fall on two straight lines that meet at Me_{75}. A discontinuity occurs in the unit-cell parameters at Me_{75} and no phase transition occurs across the scapolite series.

The structure of marialite (Me_6) and meionite (Me_{93}) refines equally well in both space groups $I4/m$ and $P4_2/n$, and similar structural results were obtained. There is no reason to refine samples close to Me_0 and Me_{100} in the higher symmetry space group $I4/m$, thereby implying transitions and forcing the T2 and T3 sites to be the same T2′ site. In space group $P4_2/n$, Me_6 and Me_{93} have ⟨T2-O⟩ and ⟨T3-O⟩ distances that not identical. Therefore, space group $I4/m$ should not be used for scapolite. We reconfirm that scapolite forms two solid solutions that meet at Me_{75}, where a discontinuity occurs in chemical composition and unit-cell parameters (Hassan and Antao, 2010), as was previously noted (Evans *et al.*, 1969; Hassan and Buseck, 1988). Moreover, there is no phase transition across the scapolite series.

ACKNOWLEDGMENT

We thank J. Post for the Me_{93} sample. Use of the Advanced Photon Source was supported by the U.S. Department of Energy, Office of Science, Office of Basic Energy Sciences, under Contract No. DE-AC02-06CH11357. This work was supported by a University of Calgary grant, a discovery grant from the National Science and Engineering Research Council of Canada, and an Alberta Ingenuity New Faculty Award.

Aitken, B. G., Evans, H. T., and Konnert, J. A. (**1984**). "The crystal-structure of a synthetic meionite," Neues Jahrb. Mineral., Abh. **149**, 309–324.

Antao, S. M., and Hassan, I. (**2002**). "Thermal behavior of scapolite $Me_{79.6}$ and $Me_{33.3}$," Can. Mineral. **40**, 1395–1401.

Antao, S. M., and Hassan, I. (**2008a**). "Increase in Al-Si and Na–Ca disorder with temperature in scapolite $Me_{32.9}$," Can. Mineral. **46**, 1577–1591.

Antao, S. M., and Hassan, I. (**2008b**). "Unusual Al-Si ordering in calcic scapolite, $Me_{79.6}$, with increasing temperature," Am. Mineral. **93**, 1470–1477.

Antao, S. M., Hassan, I., Wang, J., Lee, P. L., and Toby, B. H. (**2008**). "State-of-the-art high-resolution powder X-ray diffraction (HRPXRD) illustrated with Rietveld structure refinement of quartz, sodalite, tremolite, and meionite," Can. Mineral. **46**, 1501–1509.

Belokoneva, E. L., Sokolova, N. V., and Dorokhova, G. I. (**1991**). "Crystal structure of natural Na, Ca-scapolite—An intermediate member of the marialite-meionite series," Sov. Phys. Crystallogr. **36**, 828–830.

Belokoneva, E. L., Sokolova, N. V., and Urusov, V. S. (**1993**). "Scapolites-crystalline-structures of marialite (Ma11) and Meinite (Me88)-spatial group as a function of composition," Kristallografiya **38**, 52–57.

Chamberlain, C. P., Docka, J. A., Post, J. E., and Burnham, C. W. (**1985**). "Scapolite-alkali atom configurations, antiphase domains, and compositional variations," Am. Mineral. **70**, 134–140.

Comodi, P., Mellini, M., and Zanazzi, P. F. (**1990**). "Scapolites; variation of structure with pressure and possible role in the storage of fluids," Eur. J. Mineral. **2**, 195–202.

Deer, W. A., Howie, R. A., and Zussman, J. (**1992**). *An Introduction to the Rock-Forming Minerals*, 2nd ed. (Wiley, New York).

Evans, B. W., Shaw, D. M., and Haughton, D. R. (**1969**). "Scapolite stoichiometry," Contrib. Mineral. Petrol. **24**, 293–305.

Hassan, I., and Antao, S. M. (**2010**). "An Al-Si order and composition model for scapolite solid solutions with conformation form HRPXRD data," Acta Mineralogica-Petrographica **6**, 719.

Hassan, I., Antao, S. M., and Parise, J. B. (**2004**). "Sodalite: high temperature structures obtained from synchrotron radiation and Rietveld refinements," Am. Mineral. **89**, 359–364.

Hassan, I., and Buseck, P. R. (**1988**). "HRTEM characterization of scapolite solid solutions," Am. Mineral. **73**, 119–134.

Hassan, I., and Grundy, H. D. (**1984**). "The crystal structures of sodalite-group minerals," Acta Crystallogr., Sect. B: Struct. Sci. **40**, 6–13.

Hawthorne, F. C., and Sokolova, E. (**2008**). "The crystal chemistry of the scapolite-group minerals. II. The origin of the $I4/m \longleftarrow\longrightarrow P4_2/n$ phase transition and the nonlinear variations in chemical composition," Can. Mineral. **46**, 1555–1575.

Larson, A. C., and Von Dreele, R. B. (**2000**). "General structure analysis system (GSAS)," Los Alamos National Laboratory Report No. LAUR 86-748.

Lee, P. L., Shu, D., Ramanathan, M., Preissner, C., Wang, J., Beno, M. A., Von Dreele, R. B., Ribaud, L., Kurtz, C., Antao, S. M., Jiao, X., and Toby, B. H. (**2008**). "A twelve-analyzer detector system for high-resolution powder diffraction," J. Synchrotron Radiat. **15**, 427–432.

Levien, L., and Papike, J. J. (**1976**). "Scapolite crystal chemistry: Aluminum-silicon distributions, carbonate group disorder, and thermal expansion," Am. Mineral. **61**, 864–877.

Lin, S. B. (**1975**). "Crystal chemistry and stoichiometry of the scapolite group," Acta Geol. Taiwanica **18**, 36–48.

Lin, S. B., and Burley, B. J. (**1973a**). "Crystal structure of a sodium and chlorine-rich scapolite," Acta Crystallogr. B **29**, 1272–1278.

Lin, S. B., and Burley, B. J. (**1973b**). "The crystal structure of meionite," Acta Crystallogr. B **29**, 2024–2026.

Lin, S. B., and Burley, B. J. (**1973c**). "On the weak reflections violating body-centered symmetry in scapolites," Tschermaks Mineral. Petrogr. Mitt. **20**, 28–44.

Lin, S. B., and Burley, B. J. (**1974**). "The crystal-structure of an intermediate scapolite - wernerite," Tschermaks Mineral. Petrogr. Mitt. **21**, 196–215.

Papike, J. J., and Stephenson, N. C. (**1966**). "The crystal structure of mizzonite, a calcium- and carbonate-rich scapolite," Am. Mineral. **51**, 1014–1027.

Papike, J. J., and Zoltai, T. (**1965**). "The crystal structure of a marialite scapolite," Am. Mineral. **50**, 641–655.

Pauling, L. (**1930**). "The structure of some sodium and calcium aluminosilicates," Proc. Natl. Acad. Sci. U.S.A. **16**, 453–459.

Peterson, R. C., Donnay, G., and LePage, Y. (**1979**). "Sulfate disorder in scapolite," Can. Mineral. **17**, 53–61.

Phakey, P. P., and Ghose, S. (**1972**). "Scapolite: Observation of anti-phase domain structure," Nature (London), Phys. Sci. **238**, 78–80.

Rietveld, H. M. (**1969**). "A profile refinement method for nuclear and magnetic structures," J. Appl. Crystallogr. **2**, 65–71.

Schiebold, E., and Seumel, G. (**1932**). "Űber die kristallstruktur von skapolith," Z. Kristallogr. **81**, 110–134.

Seto, Y., Shimobayashi, N., Miyake, A., and Kitamura, M. (**2004**). "Composition and $I4/m-P4_2/n$ phase transition in scapolite solid solutions," Am. Mineral. **89**, 257–265.

Sherriff, B. L., Sokolova, E. V., Kabalov, Y. K., Jenkins, D. M., Kunath-Fandrei, G., Goetz, S., Jäger, C., and Schneider, J. (**2000**). "Meionite: Rietveld structure-refinement, ^{29}Si MAS and ^{27}Al SATRAS NMR spectroscopy, and comments on the marialite-meionite series," Can. Mineral. **38**, 1201–1213.

Sherriff, B. L., Sokolova, E. V., Kabalov, Y. K., Teertstra, D., Kunath-Fandrei, G., Goetz, S., and Jäger, C. (**1998**). "Intermediate scapolite: ^{29}Si MAS and ^{27}Al SATRAS NMR spectroscopy and Rietveld structure-refinement," Can. Mineral. **36**, 1267–1283.

Sokolova, E., and Hawthorne, F. C. (**2008**). "The crystal chemistry of the scapolite-group minerals. I. Crystal structure and long-range order," Can. Mineral. **46**, 1527–1554.

Sokolova, E. V., Gobechiya, E. R., Zolotarev, A. A., and Kabalov, Y. K. (**2000**). "Refinement of the crystal structures of two marialites from the Kukurt deposit of the east Pamirs," Crystallogr. Rep. **45**, 934–938.

Sokolova, E. V., Kabalov, Y. K., Sherriff, B. L., Teertstra, D. K., Jenkins, D. M., Kunath-Fandrei, G., Goetz, S., and Jäger, C. (**1996**). "Marialite: Rietveld structure-refinement and ^{29}Si MAS and ^{27}Al satellite transition NMR spectroscopy," Can. Mineral. **34**, 1039–1050.

Teertstra, D. K., Schindler, M., Sherriff, B. L., and Hawthorne, F. C. (**1999**). "Silvialite, a new sulfate-dominant member of the scapolite group with an Al-Si composition near the $I4/m-P4_2/n$ phase transition," Mineral. Mag. **63**, 321–329.

Teertstra, D. K., and Sherriff, B. L. (**1996**). "Scapolite cell-parameter trends along the solid-solution series," Am. Mineral. **81**, 169–180.

Toby, B. H. (**2001**). "EXPGUI, a graphical user interface for GSAS," J. Appl. Crystallogr. **34**, 210–213.

Ulbrich, H. H. (**1973a**). "Crystallographic data and refractive indices of scapolites," Am. Mineral. **58**, 81–92.

Ulbrich, H. H. (**1973b**). "Structural refinement of the Monte Somma scapolite, a 93% meionite," Tschermaks Mineral. Petrogr. Mitt. **53**, 385–393.

Wang, J., Toby, B. H., Lee, P. L., Ribaud, L., Antao, S. M., Kurtz, C., Ramanathan, M., Von Dreele, R. B., and Beno, M. A. (**2008**). "A dedicated powder diffraction beamline at the advanced photon source: Commissioning and early operational results," Rev. Sci. Instrum. **79**, 085105.

Zolotarev, A. A. (**1996**). "Once more on isomorphic schemes and isomorphic series in the scapolite group," Zap. Vses. Mineral. O-va. **125**, 69–73.

Zolotarev, A. A., Petrov, T. G., and Moshkin, S. V. (**2003**). "Peculiarities of chemical compositions of the scapolite group minerals," Zap. Vses. Mineral. O-va. **132**, 63–84.